International Journal of Engineering

Journal Homepage: www.ije.ir

Experimental and Numerical Investigation of Air Temperature Distribution inside a Car under Solar Load Condition

B. Srusti, M. B. Shyam Kumar*

School of Mechanical and Building Sciences, VIT Chennai, India

P A P E R I N F O

Paper history:
Received 13 October 2018
Received in revised form 03 May 2019
Accepted 03 May 2019

Keywords:
Solar radiation
Car Cabin Temperature
Computational Fluid Dynamics
Discrete Ordinance Radiation Model
Surface to Surface Radiation Model

A B S T R A C T

In this work both experimental and numerical analysis are carried out to investigate the effect of solar radiation on the cabin air temperature of Maruti Suzuki Celerio car parked for 90 min under solar load condition. The experimental and numerical analysis encompasses on temperature increment of air at various locations inside the vehicle cabin. The effect of 90 min exposure to the environment is simulated with the help of Discrete Ordinance (DO) and Surface to Surface (S2S) radiation models using ANSYS FLUENT 18.2. Moreover, the impacts of using different turbulence model on the accuracy of the simulation results and the comparison between steady state and transient state simulation results have also been studied. The results of the simulation are compared with the experimental data to contrast the model. The absolute average deviation in temperature predicted by DO and S2S model from the experimental data are 10.08 and 10.01%, respectively.

***doi**: 10.5829/ije.2019.32.07a.17*

NOMENCLATURE

DO	Discrete Ordinance Radiation Model	g	Acceleration Due to Gravity (m/s^2)
S2S	Surface to Surface Radiation Model	**Greek Symbols**	
DBT	Dry Bulb Temperature	k	Turbulent Kinetic Energy
P_{atm}	Atmospheric Pressure	ε	Turbulent Dissipation Rate
RNG	Renormalization Group Theory	ω	Specific Turbulent Dissipation Rate
SST	Shear Stress Transport	ρ	Density (in kg/m^3)
RTD	Resistance Temperature Detector	σ	Turbulent Prandtl Number
N_θ, N_ϕ	Solid Angles for Area Discretization	υ_t	Turbulent Eddy Viscosity
θ, ϕ	Polar and Azimuthal Angles	ε	Turbulent Dissipation Rate
AD	Average Deviation	α	Absorptivity
$\bar{u}, \bar{T}$	Mean Velocity and Temperature	τ	Transmissivity
u', T'	Fluctuating Velocity and Temperature	p	Reflectivity

1. INTRODUCTION

The cabin of the vehicle is the space where thermal discomfort is observed. The vehicle outer body is made of sheet metal which can absorb 20% to 90% of the incoming solar radiation. Solar radiation mainly comes inside the car through windshield and is partially trapped within the car. Once the passengers get into the vehicle during summer, they can experience thermal discomfort due to the high temperatures inside. According to ASHRAE Standard, 25℃ DBT (Dry Bulb Temperature) and 50% relative humidity is the desirable conditions for human comfort [1].

*Corresponding Author Email: *shyamkumar.mb@vit.ac.in* (M. B. Shyam Kumar)

Please cite this article as: B. Srusti, M. B. Shyam Kumar, Experimental and Numerical Investigation of Air Temperature Distribution inside a Car under Solar Load Condition, International Journal of Engineering (IJE), IJE TRANSACTIONS A: Basics Vol. 32, No. 7, (July 2019) 1031-1039

Simion et al. [2] examined the factors which influence thermal discomfort inside the vehicle and found out that the temperature and relative humidity are the two most important factors influencing human comfort. Another problem associated with excessive heat is heat stokes which mainly affects children and pets [3, 4]. Grundstein et al. [5] examined the cabin temperature under different meteorological conditions and found out that even in cloudy days with lower ambient temperature, the vehicle cabin temperature can reach deadly level. Currle et al. [6] investigated the effect of air vent area and air mass flux on the thermal comfort of car passenger and found that uncomfortable air draught can be observed above the head of the car passenger sitting in the front. Simulation of cabin climatic conditions are becoming very important because it can be an alternative for wind tunnel and field testing to achieve improved thermal comfort.

Neacsu et al. [7] reported the influence of solar radiation on the interior temperature of the car using THESEUS-FE 3.0. Patil et al. [8] studied the influence of solar load on rising the temperature of air inside the car using one dimensional solar heat load simulation. Sevilgen and Kilic [9] employed Surface to Surface (S2S) model and investigated the transient cooling of an automobile cabin under solar radiation and compared the results with that of the experimental data.

Moreover, the comparative study of different turbulence models and different radiation models has not been reported till date. In the present work, the results of the simulation obtained with different radiation and turbulence models are compared with that of the experimental results to examine the feasibility and accuracy of these models. Moreover, the error analysis of these parameters has also been done. A comparison is also made between the results obtained from the steady state and transient simulation, and the challenges faced while modelling the simulation. The experimental study involves monitoring the air temperature of car cabin exposed to solar radiation for 90 min. Numerical analysis involves using different radiation and turbulence models to carry out the simulations for the same 90 min and study the effect of solar radiation on the car cabin temperature. Finally, comparison between the two results will be made to check the feasibility of the proposed models.

2. CFD ANALYSIS

2. 1. Modelling and Meshing Modelling of the car is done in CATIA and imported to HYPERMESH for meshing. Figures 1 and 2 show the car dimensions and car profiles employed for modelling, respectively. Mesh-independence study has been performed to check the dependence of mesh on the results of the simulation.

First, simulations are performed with the coarser mesh and gradually the mesh density was changed to fine. All the simulations are performed with fine mesh structure. Approximately 10 million elements and nodes are generated. A volumetric aspect ratio of less than 20 and volumetric skewness of less than 0.98 is obtained. Table 1 shows mesh-independence study and error analysis. Using S2S model, the change in cabin roof temperature is considered as a benchmark for mesh-independence study. The difference in temperature of the roof when mesh type changes from medium to fine was small as compared to the change in number of elements. Hence, it can be concluded that refining mesh

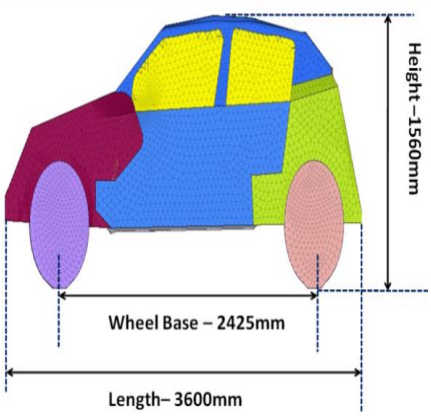

Figure 1. Car dimensions (Maruti Suzuki Celerio)

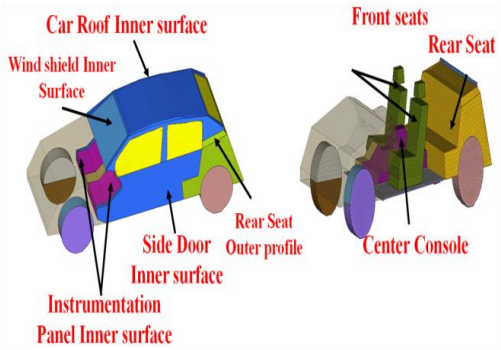

Figure 2. Car Profile

TABLE 1. Mesh Independence Study

Mesh Type	Coarse	Medium	Fine
No of Elements.	3045672	6888795	11023053
No of Nodes	467543	1028663	1638839
Roof Temp (Simulation).	50.21°C	55.13°C	56.4°C
Roof Temp (Experiment)	57.75°C	57.75°C	57.75°C
% Error	13.05%	4.5%	1.04%

further will not lead to a considerable change in the results. Figure 3 shows the fine mesh structure of the car.

2. 2. Assumptions

1. The flow is considered to be three-dimensional and incompressible
2. Air is defined as incompressible ideal gas and all the material properties are considered isotropic
3. Outlet pressure is equal to P_{atm}
4. Ambient Temperature is held constant at 35°C
5. Inner air is subjected to the transient natural convection behavior.
6. Seat features, IP panel features are neglected to reduce the complexity.
7. The IP panel, front and rear seat profile are considered as adiabatic walls.
8. The readings are taken after every 2 min intervals to avoid or minimize the effect of temperature fluctuations and sudden non-linearity in the results.

An attempt has been made to simulate the input solar radiation using the two radiation models namely the Discrete Ordinance (DO) and Surface to Surface (S2S) models available in ANSYS FLUENT 18.2. In addition, four different turbulence models namely the k-ε Realizable, k-ε Standard, k-ε RNG and k-ω SST were employed in this simulation. Both steady state and transient state simulations were performed.

2. 3. Governing Equations The governing equations namely the Continuity (Equation (1)), Momentum (Equation (2)) and Energy equations (Equation (3)) were solved using the finite volume method.

$$\frac{\partial \rho}{\partial t}+\frac{\partial\left(\rho\overline{u_i}\right)}{\partial x}=0 \tag{1}$$

$$\frac{\partial \overline{u_i}}{\partial t}+\overline{u_j}\frac{\partial \overline{u_i}}{\partial x_j}=-\frac{1}{\rho}\frac{\partial \overline{p}}{\partial x_i}+\frac{\partial}{\partial x_j}\left[\upsilon\frac{\partial \overline{u_i}}{\partial x_j}-\overline{u_i'u_j'}\right]$$
$$\text{where } \overline{u_i'u_j'}=\upsilon_t\left(\frac{\partial \overline{u_i}}{\partial x_j}+\frac{\partial \overline{u_j}}{\partial x_i}\right)-\frac{2}{3}k\delta_{ij} \tag{2}$$

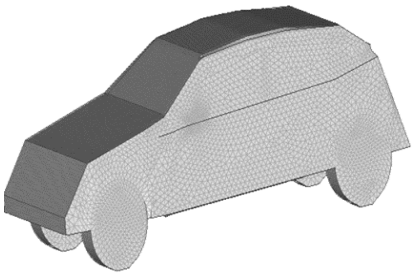

Figure 3. Fine Mesh Structure

$$\frac{\partial \overline{T}}{\partial t}+\overline{u_i}\frac{\partial \overline{T}}{\partial x_i}=\frac{\partial}{\partial x_i}\left[\alpha\frac{\partial \overline{T}}{\partial x_i}-\overline{u_i'T'}\right]$$
$$\text{where}\,\overline{u_i'T'}=\alpha_t\frac{\partial \overline{T}}{\partial x_i}\,\text{and}\,\alpha_t=\frac{\upsilon_t}{\sigma_t} \tag{3}$$

Here ρ is the density, μ the dynamic viscosity, $\overline{u}$ the mean velocity, u' the fluctuating velocity component, $\overline{p}$ the mean pressure, T temperature, and t the time. Subscripts i, j are the x, y, z position tensor, α is the thermal diffusivity, υ_t the turbulent eddy viscosity and σ_t the turbulent Prandtl number.

2. 3. 1. k-epsilon Realizable Model The two transport equations [10] are for turbulent kinetic energy (k):

$$\frac{\partial}{\partial t}(\rho k)+\frac{\partial}{\partial x_j}(\rho k u_j)=\frac{\partial}{\partial x_j}\left[\left(\mu+\frac{\mu_t}{\sigma_k}\right)\frac{\partial k}{\partial x_j}\right]+ G_k+G_b-\rho\varepsilon-Y_M+S_k \tag{4}$$

For turbulent dissipation rate (ε):

$$\frac{\partial}{\partial t}(\rho \varepsilon)+\frac{\partial}{\partial x_j}(\rho \varepsilon u_j)=\frac{\partial}{\partial x_j}\left[\left(\mu+\frac{\mu_t}{\sigma_\varepsilon}\right)\frac{\partial \varepsilon}{\partial x_j}\right]+ \rho C_1 S_\varepsilon-\rho C_2\frac{\varepsilon^2}{k+\sqrt{\upsilon\varepsilon}}+C_{1\varepsilon}\frac{\varepsilon}{k}C_{3\varepsilon}G_b+S_\varepsilon \tag{5}$$

Here G_k and G_b represent the generation of turbulence kinetic energy due to the mean velocity gradients and buoyancy respectively. Y_M represent the contribution of the fluctuating dilation in compressible turbulence to the overall dissipation rate, C_2, $C_{1\varepsilon}$ are constants with σ_k and σ_ε are the turbulent Prandtl numbers for k and ε. S_k and S_ε are user-defined source terms.

2. 3. 2. k-epsilon Standard Model The two transport equations [10] are for turbulent kinetic energy:

$$\frac{\partial}{\partial t}(\rho k)+\frac{\partial}{\partial x_i}(\rho k u_i)=\frac{\partial}{\partial x_j}\left[\left(\mu+\frac{\mu_t}{\sigma_k}\right)\frac{\partial k}{\partial x_j}\right]+ G_k+G_b-\rho\varepsilon-Y_M+S_k \tag{6}$$

Here μ_t is the turbulent/eddy viscosity computed using

$$\mu_t=\rho C_\mu\frac{k^2}{\varepsilon}$$

For turbulent dissipation rate:

$$\frac{\partial}{\partial t}(\rho \varepsilon)+\frac{\partial}{\partial x_j}(\rho \varepsilon u_j)=\frac{\partial}{\partial x_j}\left[\left(\mu+\frac{\mu_t}{\sigma_\varepsilon}\right)\frac{\partial \varepsilon}{\partial x_j}\right]+ \rho C_1 S_\varepsilon-\rho C_2\frac{\varepsilon^2}{k+\sqrt{\upsilon\varepsilon}}+C_{1\varepsilon}\frac{\varepsilon}{k}C_{3\varepsilon}G_b+S_\varepsilon \tag{7}$$

2. 3. 3. k-epsilon RNG Model The two transport equations [10] are:
For turbulent kinetic energy:

$$\frac{\partial}{\partial t}(\rho k)+\frac{\partial}{\partial x_i}(\rho k u_i)=\frac{\partial}{\partial x_j}\left(\alpha_k \mu_{eff}\frac{\partial k}{\partial x_j}\right)+ G_k+G_b-\rho\varepsilon-Y_M+S_k \quad (8)$$

For turbulent dissipation rate:

$$\frac{\partial}{\partial t}(\rho \varepsilon)+\frac{\partial}{\partial x_i}(\rho \varepsilon u_i)=\frac{\partial}{\partial x_j}\left(\alpha_\varepsilon \mu_{eff}\frac{\partial \varepsilon}{\partial x_j}\right)+ C_{1\varepsilon}\frac{\varepsilon}{k}(G_k+C_{3\varepsilon}G_b)-C_{2\varepsilon}\rho\frac{\varepsilon^2}{k}-R_\varepsilon+S_\varepsilon \quad (9)$$

2. 3. 4. k-omega SST Model The two transport equations [10] are for turbulent kinetic energy (k):

$$\frac{\partial}{\partial t}(\rho k)+\frac{\partial}{\partial x_i}(\rho k u_i)=\frac{\partial}{\partial x_j}\left(\Gamma_k\frac{\partial k}{\partial x_j}\right)+ G_k-Y_k+S_k \quad (10)$$

For specific dissipation rate (ω):

$$\frac{\partial}{\partial t}(\rho \omega)+\frac{\partial}{\partial x_i}(\rho \omega u_i)=\frac{\partial}{\partial x_j}\left(\Gamma_\omega\frac{\partial \omega}{\partial x_j}\right)+G_\omega- Y_\omega+D_\omega+S_\omega \quad (11)$$

Complete details of the above four turbulence models can be found in [10] along with the physical meaning of the different terms and its computations. The values of the different constants can be found in the same reference as well.

2. 4. Solar Load Model Various solar models are available in ANSYS FLUENT 18.2 consisting of solar ray tracing and solar radiation model. In the present study, only Discrete Ordinance (DO) and Surface to Surface (S2S) models are considered.

2. 4. 1. Discrete Ordinance (DO) Model DO model solves the RTE for a finite number of discrete solid angles, each associated with a direction fixed in the global Cartesian coordinate (x,y,z). The fineness of the rays can be controlled through angular discretization. The equation for DO model are as follows [10]:

$$\nabla.\left(I(\vec{r},\vec{s})\vec{s}\right)+(a+\sigma_s)I(\vec{r},\vec{s})=an^2\frac{\sigma T^4}{\pi}+\frac{\sigma_s}{4\pi}\int_0^{4\pi} I(\vec{r},\vec{s}')\Phi(\vec{s}.\vec{s}')d\Omega' \quad (12)$$

The total intensity $I(\vec{r},\vec{s})$ in each direction $\vec{s}$ and at position $\vec{r}$ is computed using:

$$I(\vec{r},\vec{s})=\sum_k I_{\lambda_k}(\vec{r},\vec{s})\Delta\lambda_k$$

2. 4. 2. Surface to Surface (S2S) Model The surface to surface model is used for calculating radiation exchange in an enclosure of diffuse surface. The energy exchanged between the two surfaces mainly depends on the view factor. Applying the conservation of energy equation we get [10]:

$$\alpha+\tau+p=1 \quad (13)$$

where α = absorptivity which is equal to Ɛ = emissivity and p = transmissivity in surface to surface model.

The energy flux which leaves the surface is composed of directly reflected and emitted energy. The outgoing reflected energy is the function of incident energy flux from all the directions.

$$q_{out,k}=\varepsilon_k\sigma T_k^4+\rho_k q_{in,k} \quad (14)$$

where $q_{out,k}$ and $q_{in,k}$ are the energy flux leaving the surface and that incident on the surface, respectively.

2. 5. Solar Ray Tracing Solar ray tracing uses both positioning vector and two illumination parameters to set solar radiation intensities that represent the solar load. To give the direction and magnitude of intensity of the solar radiation, the solar calculator is used. Absorptivity and transmissivity are defined for all the solid materials. Glass is modelled as semi-transparent object while other solid components are modelled as opaque. Some of the materials which are not defined in the ANSYS FLUENT namely the foam, rubber and plastics are defined using create material option. Figure 4 shows the longitude and latitude of the place.

Here, experiments have been performed during the same time that the solar calculator has predicted. Accurate prediction of solar radiation is necessary to calculate the temperature rise of the air inside the cabin. Tolabi et al. [11] formulated a new technique to predict the global radiation forecast using bees algorithm. However in the current simulation the radiation intensity will be predicted internally by ANSYS FLUENT.

3. EXPERIMENTAL SETUP

The schematic diagram of car is shown in Figure 5. The experimental setup comprises of RTD sensors namely Pt - 100(1/5 DIN class B) Temperature sensor which are placed at various locations inside the car (Figure 6).

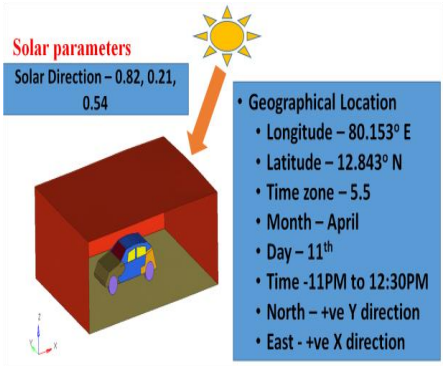

Figure 4. Solar Calculator

The RTD sensors are attached with the 16 channel data logger to record the temperature. All temperature sensors were previously calibrated for the range 10°C to 80°C in MICROCAL T100 equipment with an accuracy of 0.1°C. Solar radiation is measured using the Standard Pyranometer manufactured by TENMARS ELECTRONICS CO., LTD having an accuracy of ±10W/m^2.

4. RESULTS AND DISCUSSION

The experiments showed that the temperature is highest at the roof and lowest at the feet. There is a gradual decrease in the temperature of air from roof towards the feet. The average air temperature at the roof is 58 °C at 12:30 PM. The difference between the average air temperatures at the roof and at the feet is 22°C. Figure 7 shows the air temperature at different locations inside the car cabin at different time steps, when the car is exposed to 90 min of solar radiation. Figure 8 shows the solar radiation intensity data measured by the pyranometer during the time of experiment.

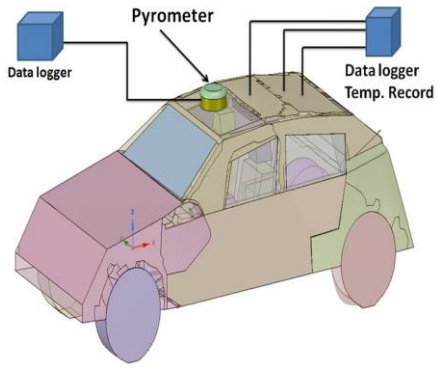

Figure 5. Schematic Diagram

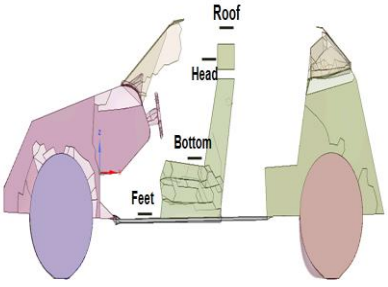

Figure 6. Positioning of RTD sensors at various locations

4. 1. Steady State Analysis Table 2 shows the details of the simulation. Steady state analysis is first done using different radiation and turbulence models. Here, only DO and S2S radiation models are considered for the simulations. Other models like Roseland and P1 radiation models are not considered for the simulation because these models are used only with optically thick mediums [10].

Figure 9 shows the temperature of air at various locations obtained from S2S steady state analysis using different turbulence models. It is found that the steady state simulation is unable to give accurate results for all the turbulence models. As S2S model failed to provide

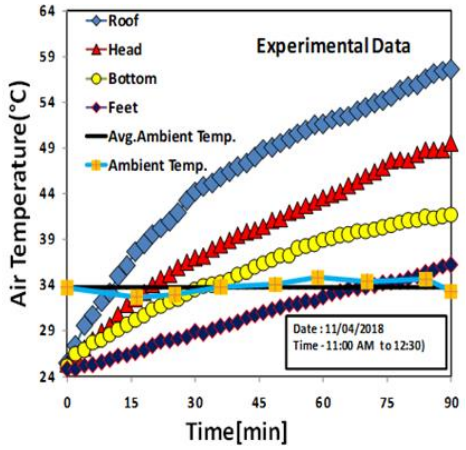

Figure 7. Air Temperature at different intervals of time

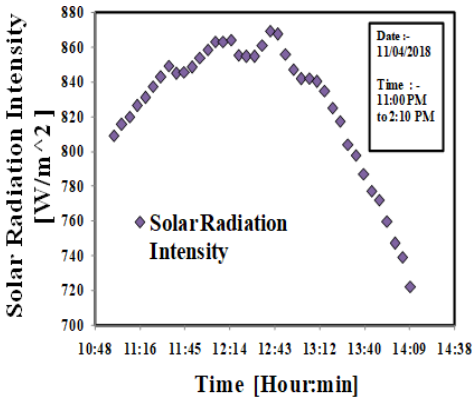

Figure 8. Solar Radiation intensity

TABLE 2. Simulation Methods

Radiation Models	DO Model / S2S Model
Turbulence Model	k-ε RNG, k-ε Realizable, k-ω SST, k-ε Standard
Simulation Type	Steady State / Transient (90 min)
Discretization Method	Solver – SIMPLE Algorithm Pressure – Body Weighted Average Velocity – Second Order Energy – Second order DO radiation – First order
Gravity	-ze direction(-9.81m/s^2)
Convergence Criteria	Continuity /Momentum – 1e-04 Energy – 1e-06 DO – 1e-06
Time Step	0.25s

accurate results under steady state condition, the simulation is now done using DO model. Like S2S model steady state simulation DO model also faces convergence issues and the simulation is made to converge using under relaxation factors.

Figure 10 shows the air temperature predicted by simulation when using Discrete Ordinance (DO) model for different turbulence models. The steady simulation using both S2S and DO models over predicted the temperature values for all turbulence models considered in present study.

Figures 11 and 12 shows the air temperature contour along the plane ~10 cm away from the window obtained from the steady simulation using S2S and DO radiation models and k-ε realisable model with scalable wall function, respectively. It is thus found that the steady state simulation is unable to provide the accurate results using both radiation models and for the entire turbulence models considered in present study. This is due to the amount of time taken to reach equilibrium/steady state ranging from 20 min to 60 min [5].

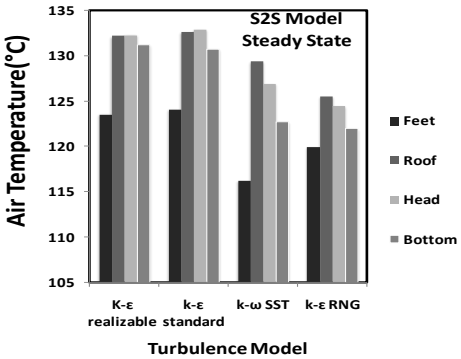

Figure 9. Air temperature at various locations

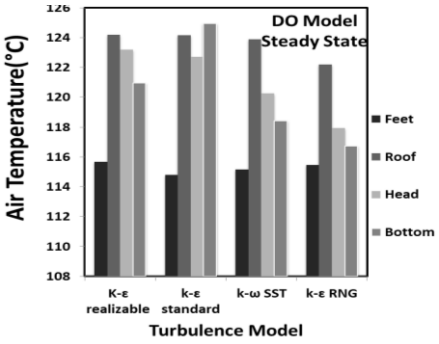

Figure 10. Air temperature at various locations

4. 2. Transient Simulation As steady state simulation failed to provide the accurate results, a transient simulation was performed using DO model with Realisable k-ε as the turbulence model. The simulation was run on HPC (High Performance Computing) for faster processing. The number of parallel processors was set to 25. The 90 min solar radiation simulation was run for almost 30 days.

Figure 13 shows the air temperature distribution along the plane ~10 cm away from the window at different intervals of time predicted by simulation using DO model under transient state condition. Figure 15 shows temperature at different locations predicted by the simulation at different intervals of time.

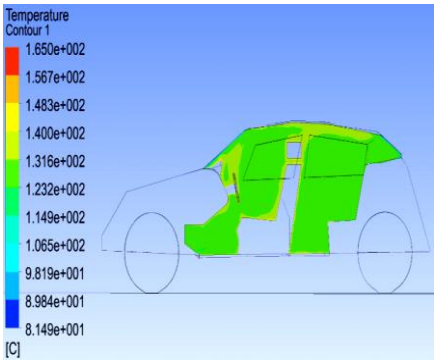

Figure 11. Air temperature distribution along the plane

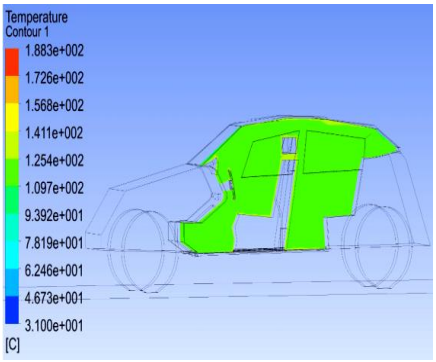

Figure 12. Air temperature distribution along the plane

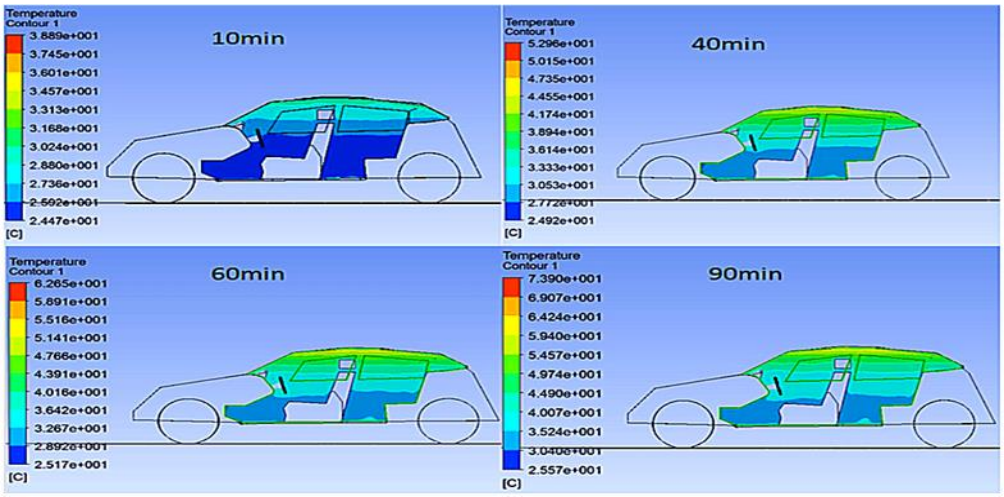

Figure 13. Temperature contours at different intervals of time (DO Model)

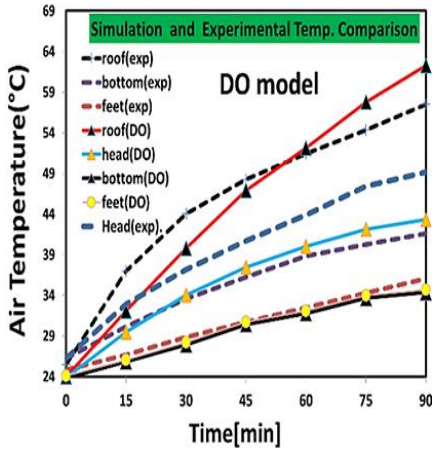

Figure 15. Air temperature at different intervals of time

The temperature predicted at roof and at 90th min is ~ 61°C which is 3°C greater than the experimental roof temperature. The difference between roof temperature and feet temperature predicted by DO model at 90 min is 26.61°C which is 5.06°C greater than experimental data. Now transient simulation is performed using S2S model. This took almost 2 days to complete the run which shows that S2S model is computationally less expensive than DO Model. This may be due to the fact that S2S model assume all the surfaces are already grey and diffuse so that any emission, scattering of the medium are ignored and only surface and boundaries are considered for radiation This means that the mediums are non-participating to the radiations. S2S model solves radiation equations based on view factor calculation. N equations are solved for N surfaces. DO model uses the different approach to solve radiation problem. It solves the transport equation similar to flow and energy equation. Each DO has a Solid angle or area discretization given by Nθ and Nφ direction that represents the radiation within a solid angle**.** The whole geometry is discretized into many solid angles. For each solid angles or band 8*NϕNθ equations are solved for 3D geometry which makes it computationally more expensive than S2S. DO model accounts for emission and scattering of the medium that means the medium is a participating media**.** Figure 14 shows the air temperature distribution along the plane ~ 10 cm away from the window at different intervals of time predicted by simulation using S2S model under transient state condition. Figure 16 shows that the temperature predicted at the roof is 1.35°C lesser than experimental data.

The difference between roof and feet temperatures at 90 min is 22.1°C which is 0.64°C greater than experimental data. This means that Surface to Surface (S2S) model predicts the temperature data with better accuracy compared to DO model. Both the models however are unable to predict the bottom air temperature with commendable accuracy. Table 3 compares the experimental and numerical results for temperature obtained at the four locations inside the car along with the error analysis.

Temperature of the air increases very rapidly when the car is parked under solar load condition. Measures should be taken to decrease the temperature of air inside the car. One such measure is to incorporate Phase Change Material (PCM) inside the car [12]. Phase change materials are already proved useful in many applications [13]. The effect of phase change material in reducing the temperature of air inside the car will be discussed in another paper.

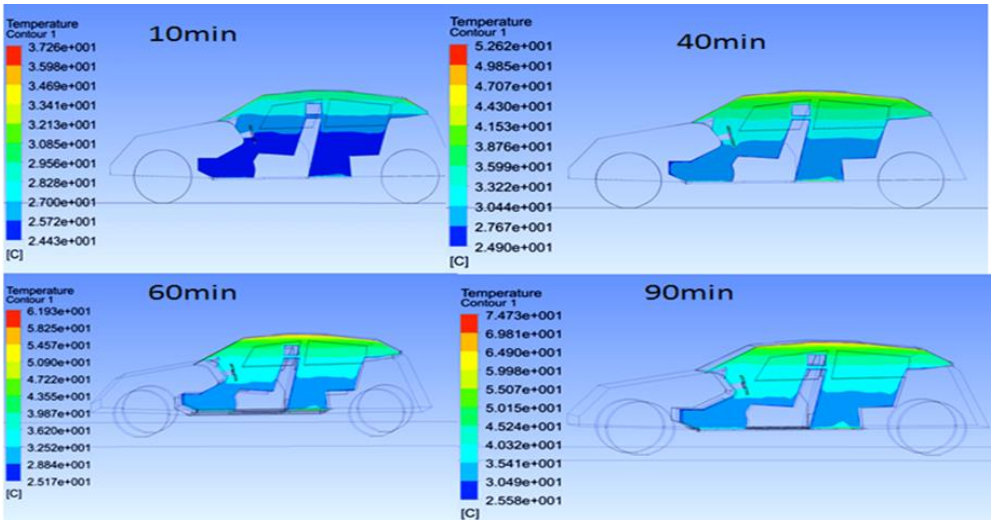

Figure 14. Temperature contours at different intervals of time (S2S Model)

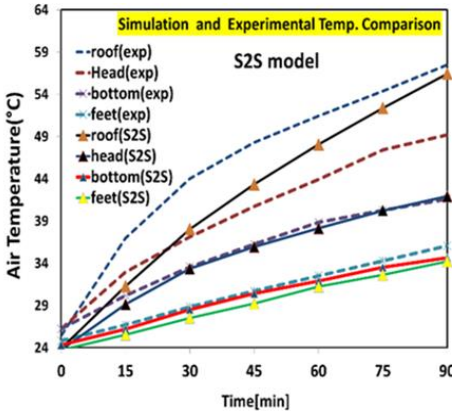

Figure 16. Air temperature at different intervals of time

TABLE 3. Comparison of experimental and numerical values for temperature at different locations

Location	Measured Values	Predicted Values (DO)	Predicted Values (S2S)	AD (DO) %	AD (S2S) %
Roof	57.75°C	61.28°C	56.4°C	6.11	2.33
Head	49.54°C	43.33°C	41.9°C	12.53	15.4
Bottom	41.66°C	34.37°C	34.65	17.5	16.82
Feet	36.2°C	34.67°C	34.21	4.2	5.5

5. CONCLUSIONS

The temperature of air inside the vehicle can increase to the level which causes discomfort to the passengers when the car is parked in sunlight for a shorter duration of time. Experimental and numerical investigation proved that there is ~ 30°C increase in the temperature of the air when the car is parked for 90 min under solar load conditions. Steady state simulations failed to predict the correct values of temperature for radiation and turbulence models that were considered for simulations. This is due to the fact that steady state simulations ignore many of the cross terms and higher order terms dealing with time. Transient simulation predicts the experimental data with 90% accuracy for both the radiation models. The Surface to Surface model is found to be computationally less expensive than DO model. However, the deviation in the simulation results can be reduced by fine tuning the material properties according to the experimental material properties.

6. REFERENCES

1. American Society of Heating, Refrigerating, Air-Conditioning Engineers, and American National Standards Institute. Thermal environmental conditions for human occupancy. American Society of Heating, Refrigerating and Air-Conditioning Engineers, 2004.
2. Simion, Mihaela., Socaciu, Lavinia., Unguresan, Paula., "Factors which influence the thermal comfort inside of vehicles", ***Energy Procedia,*** Vol. 85, (2016), 472-480.
3. Catherine, McLaren., Jan, Null., James, Quinn., "Heat stress from enclosed vehicles: moderate ambient temperatures causes significant temperature rise in enclosed vehicles", ***Pediatrics***, Vol. 116, No. 1, (2005), 109–112.
4. Dadour, I.R., Almanjahie, I., Fowkes, N.D., Keady, G., Vijayan, K., "Temperature variations in a parked vehicle", ***Forensic Science International***, Vol. 207, No. 1-3, (2011), 205–211.

5. Grundstein, Andrew., Meentemeyer, Vernon., Dowd, John., "Maximum vehicle cabin temperatures under different meteorological conditions", ***International Journal of Biometeorology***, Vol. 53, No. 3, (2009), 255–261.
6. Currle, J. and Maue, J., "Numerical Study of the Influence of Air Vent Area and Air Mass Flux on the Thermal Comfort of Car Occupants", ***SAE Technical Paper***, 2000-01-0980.
7. Neacsu, C.A., Ivanescu, M., Tabacu, I., "The Influence of the Solar Radiation on the Interior Temperature of the Car", 2009, Paper E09B108, https://www.theseus-fe.com/resources/publications.
8. Patil, Aniket., Radle, Manoj., Shome, Biswadip., Ramachandran, S., "One-Dimensional Solar Heat Load Simulation Model for a Parked Car", ***SAE Technical Paper,*** 2015-01-0356.
9. Sevilgen, Gokhan., and Kilic, Muhsin., "Investigation of Transient Cooling of an Automobile Cabin with a virtual manikin under solar radiation", ***Thermal Science***, Vol. 17, No. 2, (2013), 397-406.
10. ***ANSYS FLUENT 12.0 Theory Guide***, http://www.afs.enea.it/project/neptunius/docs/fluent/html/th/main_pre.htm
11. Tolabi, H.B., Moradib, M. and Tolabia, F.B., "New technique for global solar radiation forecast using bees algorithm", ***International Journal of Engineering – Transactions B: Applications***, Vol. 26, No. 11, (2013), 1385-1392.
12. Jadidi, A. M. and Jadidi, M., "An algorithm based on predicting the interface in phase change materials", ***International Journal of Engineering - Transactions B: Applications***, Vol. 31, No. 5 (2018), 799-804.
13. Sadafi, M., Hosseini, R., Safikhani, H., Bagheri, A. and Mahmoodabadi, M., "Multi-objective optimization of solar thermal energy storage using hybrid of particle swarm optimization, multiple crossover and mutation operator", ***International Journal of Engineering – Transactions B: Applications***, Vol. 24, No. 4, (2011), 367-376**.**

Experimental and Numerical Investigation of Air Temperature Distribution inside a Car under Solar Load Condition

B. Srusti, M. B. Shyam Kumar

School of Mechanical and Building Sciences, VIT Chennai, India

P A P E R I N F O

Paper history:
Received 13 October 2018
Received in revised form 03 May 2019
Accepted 03 May 2019

Keywords:
Solar radiation
Car Cabin Temperature
Computational Fluid Dynamics
Discrete Ordinance Radiation Model
Surface to Surface Radiation Model

چکیده

در این کار هر دو روش تجربی و عددی برای بررسی اثر تابش خورشیدی بر دمای هوای کابین خودروی مروتی سوزوکی سلئریو پارک شده به‌مدت ۹۰ دقیقه تحت شرایط تابش خورشیدی انجام شده است. تحلیل آزمایشی و عددی شامل افزایش دمای هوا در مکان‌های مختلف داخل کابین خودرو است. تاثیر ۹۰ دقیقه حضور در معرض محیط با کمک مدل-های تابشی دیجیتال (DO) و سطح به سطح (S2S) با استفاده از ANSYS FLUENT 18.2 شبیه سازی شده است. علاوه بر این، اثرات استفاده از مدل آشفتگی‌های مختلف بر دقت نتایج شبیه‌سازی‌شده از طریق مقایسه‌ی نتایج حالت شبیه‌سازی و حالت پایدار و حالت گذار نیز بررسی شده است. میانگین انحراف مطلق در دمای پیش‌بینی‌شده توسط DO و S2S از داده‌های تجربی به ترتیب ۱۰/۰۸ و ۱۰/۰۱ درصد است.

***doi**: 10.5829/ije.2019.32.07a.17*